When sinks become sources: Adaptive colonization in asexuals

Guillaume Martin, Y. Anciaux, J. Papaïx, L. Roques, Florian Lavigne

When sinks become sources: adaptive colonization in asexuals.

F Lavigne[a,b,c], G Martin[c,*], Y Anciaux[c,d], J Papaïx[a] and L Roques[a,*]

[a] BioSP, INRA, 84914, Avignon, France

[b] Aix Marseille Univ, CNRS, Centrale Marseille, I2M, Marseille, France

[c] ISEM (UMR 5554), CNRS, 34095, Montpellier, France

[d] BIRC, Aarhus University, C.F. Møllers Allé 8, DK-8000 Aarhus C, Denmark

*Corresponding authors: guillaume.martin@umontpellier.fr and lionel.roques@inra.fr

Abstract

The establishment of a population into a new empty habitat outside of its initial niche is a phenomenon akin to evolutionary rescue in the presence of immigration. It underlies a wide range of processes, such as biological invasions by alien organisms, host shifts in pathogens or the emergence of resistance to pesticides or antibiotics from untreated areas.

We derive an analytically tractable framework to describe the evolutionary and demographic dynamics of asexual populations in a source-sink system. We analyze the influence of several factors on the establishment success in the sink, and on the time until establishment. To this aim, we use a classic phenotype-fitness landscape (Fisher's geometrical model in n dimensions) where the source and sink habitats have different phenotypic optima.

In case of successful establishment, the mean fitness in the sink follows a typical four-phases trajectory. The waiting time to establishment is independent of the immigration rate and has a "U-shaped" dependence on the mutation rate, until some threshold where lethal mutagenesis impedes establishment and the sink population remains so. We use these results to get some insight into possible effects of several management strategies.

1 Introduction

Most natural populations are spread over a heterogeneous set of environments, to which local subpopulations may be more or less adapted. When these populations exchange migrants we can define "source" and "sink" populations. Source populations, where the local genotypes have positive growth rate, are self-sustained and can send migrants to the rest of the system. They may be connected to sink populations, where local genotypes are so maladapted that they have negative growth rates (Pulliam, 1988). A recent review (Furrer and Pasinelli, 2016) showed that empirical examples of sources and sinks exist throughout the whole animal kingdom. In the absence of any plastic or evolutionary change, source-sink systems are stable, with the sources being close to their carrying capacity and the sinks being only maintained by incoming maladapted migrants. In the literature, different source-sink systems have been categorized by their pattern of immigration and emigration (see Fig. 1 in Sokurenko et al. (2006) and Table 1 in Loreau et al. (2013)). Black-hole sinks, from which emigration is negligible, are the canonical model for studying the invasion of a new environment, outside of the initial species niche (Gomulkiewicz et al., 1999; Holt et al., 2003, 2004). We hereafter simply use the term "sink", when in fact referring to a black-hole sink population. The demographic and evolutionary process leading to the invasion of a sink is akin to evolutionary rescue in the presence of immigration. It underlies a wide range of biological processes: invasion of new habitats by alien organisms (Colautti et al., 2017), host shifts in pathogens or the emergence of resistance to pesticides or antibiotics, within treated areas or patients (discussed e.g. in Jansen et al. (2011) and Sokurenko et al. (2006)). The issues under study in these situations are the likelihood and timescale of successful invasions (or establishment) of sinks from neighboring source populations. "Establishment" in a sink is generally considered successful when the population is self-sustaining in this new environment, even if immigration was to stop (e.g., Blackburn et al., 2011, for a definition of this concept in the framework of biological invasions).

A rich theoretical literature has considered the effects of demography and/or evolution in populations facing a heterogeneous environment connected by migration, both in sexuals (e.g., Kirkpatrick and Barton, 1997) and asexuals (e.g., Débarre et al., 2013). The source-sink model is a sub-case of this general problem, that has received particular attention (for a review, see Holt et al., 2005): below, we quickly summarize the relevance and key properties of source-sink models. The asymmetric migration (from source to sink alone), characteristic of black-hole sinks, provides a key simplification, while remaining fairly realistic over the early phase of invasion, where success or failure

is decided. For the same reason, some models further ignore density-dependent effects in the sink, although both high (logistic growth) and/or low (Allee effect) densities could further impact the results (discussed in Holt, 2009).

Some source-sink models (e.g., Drury et al., 2007; Garnier et al., 2012), focus on detailed demographic dynamics, in the absence of any evolutionary forces. These forces (selection, mutation, migration, drift and possibly recombination/segregation) can greatly alter the outcome. They may yield both local adaptation or maladaptation, favoring or hindering (respectively) the ultimate invasion of the sink ("adaptive colonization", Gomulkiewicz et al., 2010), however harsh. In this context, mutation and migration are double edged swords, both increasing the local variance available for selection but generating mutation and migration loads, due to the adverse effects of deleterious mutations and maladapted migrant inflow (resp.). For a review of the ambivalent effects of mutation and migration see e.g., (Lenormand, 2002) and (Débarre et al., 2013). Disentangling the complex interplay of these forces with demographic dynamics is challenging, and modelling approaches have used various ecological simplifications: e.g. no age or stage structure, constant stress, constant migration rate.

The associated evolutionary processes are also simplified. As for evolutionary rescue models (discussed in Alexander et al., 2014), evolutionary source-sink models may be divided into two classes, based on the presence or absence of context-dependence in the genotype-fitness map they assume (Gomulkiewicz et al., 2010). In context-independent models, fitness in the sink is additively determined by a single or a set of freely recombining loci, and adaptation occurs by directional selection on fitness itself (Gomulkiewicz et al., 2010; Barton and Etheridge, 2017). In context-dependent models, which arguably forms the vast majority of source-sink models, fitness is assumed to be a concave function (typically quadratic or Gaussian) of an underlying phenotype, with the source and sink environments corresponding to alternative optima for this phenotype (e.g., Holt et al., 2003, 2004). Such nonlinear phenotype-fitness maps, with environment dependent optima, generate context-dependent interactions for fitness (epistasis and genotype x environment or "G x E" interactions): the effect of a given allele depends on the genetic and environmental background in which it is found. These models reproduce observed empirical patterns of mutation fitness effects across backgrounds (Martin et al., 2007; MacLean et al., 2010; Trindade et al., 2012), reviewed in (Tenaillon, 2014). However, their analysis is more involved. Most analytical treatments have thus relied on stationarity assumptions: e.g. describing the ultimate (mutation-selection-migration) equilibrium in asexuals (Débarre et al., 2013), or assuming a constant genetic variance and Gaussian distribution for the underlying trait in sexuals (e.g., Gomulkiewicz et al.,

1999; Holt et al., 2004). While numerical explorations (by individual-based simulations) often relax these stationarity assumptions, they are necessarily bound to study a limited set of parameter value combinations.

In this paper, we explore a complementary scenario: a source-sink system, out of equilibrium, in an asexual population. The focus on asexuals is intended to better capture pathogenic microorganisms or microbial evolution experiments. We ignore density-dependence by assuming that it is negligible before and during the critical early phase of the sink invasion. Considering asexuals and density-independent populations implies that several complex effects of migration (both genetic and demographic) can be ignored. Because migrants do not hybridize/recombine with locally adapted genotypes or use up limiting resources, the maladaptive effects of migration are limited. Migration meltdown and gene swamping (see Lenormand, 2002) are thus expected to be absent. This simplification allows to analytically track out-of-equilibrium dynamics, in this context-dependent model (with epistasis and G x E).

More precisely, we study the transient dynamics of a sink under constant immigration from a source population at mutation-selection balance and a sink initially empty. We use the classic quadratic phenotype-fitness map with an isotropic version of Fisher's geometrical model (FGM) with mutation pleiotropically affecting n phenotypic traits. We use a deterministic approximation (as in Martin and Roques, 2016) that neglects stochastic aspects of migration, mutation and genetic drift, but tracks the full distribution of fitness and phenotypes. Under a weak selection strong mutation (WSSM) regime, when mutation rates are large compared to mutation effects, we further obtain an analytically tractable coupled partial-ordinary differential equation (PDE-ODE) model describing the evolutionary and demographic dynamics in the sink. This framework allows us to derive analytic formulae for the demographic dynamics and the distribution of fitness, at all times, which we test by exact stochastic simulations. We investigate the effect of demographic and evolutionary parameters on the establishment success, on the establishment time, and on the equilibrium mean fitness in the sink. In particular, we focus on the effects of the immigration rate, the habitat difference (maladaptation of the optimal source phenotype in the sink environment), and mutational parameters (rate, phenotypic effects and dimension n).

2 Methods

Throughout this paper, we follow the dynamics of the fitness distribution of the individuals in the sink environment. We consider a population evolving in continuous

time. Consistently, we focus on Malthusian fitness m (hereafter "fitness"): the expected growth rate (over stochastic demographic events) of a given genotypic class, per arbitrary time units. Absolute Malthusian fitnesses r are therefore (expected) growth rates, and without loss of generality, m is measured relative to that of the phenotype optimal in the sink, with growth rate $r_{\max}$. We thus have $m = r - r_{\max}$, and the mean absolute fitness $\overline{r}(t)$ and mean relative fitness $\overline{m}(t)$, at time t, satisfy:

$$\overline{r}(t) = r_{\max} + \overline{m}(t).$$

We use a *deterministic approximation* which neglects variations among replicate populations. Under this approximation, $\overline{r}(t)$ (respectively $\overline{m}(t)$), the mean absolute (resp. relative) fitness within each population can be equated to their expected values (across stochastic events). In general, the bar $\overline{\ }$ denotes averages taken over the sink population. The main notations are summarized in Table 1. Note that the reader who is not familiar with the mathematical formalism used in this paper can safely skip most formulae in the main text, as they are also verbally explained and/or illustrated with figures.

2.1 Demographic model and establishment time t_0

In our simple scenario without density-dependence, evolutionary and demographic dynamics are entirely coupled by the mean growth rate $\overline{r}(t)$. We consider a sink population receiving on average d individuals per unit time by immigration. Under the deterministic approximation, the population size dynamics in the sink environment are therefore given by:

$$N'(t) = \overline{r}(t)\, N(t) + d, \tag{1}$$

with $N'(t)$ the derivative of N with respect to t at time t.

In the absence of adaptation, $\overline{r}$ is constant, leading to an equilibrium population size $N = d/(-\overline{r})$ when $\overline{r} < 0$, as mentioned above. When genetic adaptation is taken into account, we need further assumptions to describe the dynamics of $\overline{r}(t)$ in the sink.

We always assume that the new environment is initially empty ($N(0) = 0$) and that the individuals from the source are, on average, maladapted in the sink ($\overline{r}(0) < 0$). Following a classic definition (Blackburn et al., 2011), we define the establishment time t_0 as the first time when the growth rate of the sink becomes positive in the absence of immigration. This means that, from time t_0, the sink population is self-sustaining in the absence of immigration and further adaptation. By definition (assuming that $\overline{r}$ is

Notation	Description
n	number of pleiotropic phenotypes
$\mathbf{x}$	(breeding value for) phenotype of a given genotype
$\mathbf{x}^*$	Optimal phenotype (source)
d	Immigration rate
U	Genomic mutation rate
λ	Mutational variance per trait
μ	$\sqrt{U\,\lambda}$
m	Malthusian fitness in the sink, relative to a genotype optimal in the sink
m_D	Habitat difference (fitness distance between source and sink optima)
r_D	Decay rate (minus growth rate), in the sink, of a genotype optimal in the source $r_D = m_D - r_{\max}$
m_{source}	Fitness of the migrants in the source
m_{migr}	Fitness of the migrants in the sink
p_{migr}	Probability density of m_{migr}
$r_{\max}$	Maximum absolute fitness (sink)
r	Absolute Malthusian fitness: genotypic growth rate $r = r_{\max} + m$
$N(t)$	Population size at time t
$\overline{m}(t)$	Mean relative fitness
$\overline{r}(t)$	Mean absolute fitness: mean growth rate of the population $\overline{r}(t) = r_{\max} + \overline{m}(t)$
t_0	Establishment time
$C_t(z)$	Cumulant generating function of the relative fitness distribution in the sink

Table 1: **Main notations**

continuous), t_0 satisfies $\overline{r}(t_0) = 0$. Depending on the behavior of $\overline{r}(t)$, t_0 may therefore be finite (successful establishment) or infinite (establishment failure).

2.2 Fisher's geometric model

We use Fisher's geometric model (FGM) to describe the relationships between genotypes, phenotypes and fitnesses in each environment. This phenotype-fitness landscape model generates a coupling between habitat difference, the distribution of fitnesses among migrants from the source and that among *de novo* random mutants arising in the sink (Anciaux et al., 2018).

Phenotype-fitness relationships in the two environments. The FGM assumes that each genotype is characterized by a given breeding value for phenotype at n traits (hereafter simply denoted 'phenotype'), namely a vector $\mathbf{x} \in \mathbb{R}^n$. Each environment (the source and the sink) is characterized by a distinct phenotypic optimum. An optimal phenotype in the sink has maximal absolute fitness $r_{\max}$ (relative fitness $m = 0$) and sets the origin of phenotype space ($\mathbf{x} = 0$). Fitness decreases away from this optimum. Following the classic version of the FGM, Malthusian fitness is a quadratic function of the breeding value $r(\mathbf{x}) = r_{\max} - \|\mathbf{x}\|^2/2$ and $m(\mathbf{x}) = -\|\mathbf{x}\|^2/2$.

In the source, due to a different phenotype optimum $\mathbf{x}^* \in \mathbb{R}^n$, the relative fitness is $m^*(\mathbf{x}) = -\|\mathbf{x} - \mathbf{x}^*\|^2/2$. As the population size is kept constant in the source (see below), only relative fitness matters in this environment. The habitat difference $m_D > 0$ is the fitness distance between source and sink optima:

$$m_D = -m(\mathbf{x}^*) = \|\mathbf{x}^*\|^2/2. \tag{2}$$

For consistency with previous work, we denote r_D the decay rate, in the sink, of a population composed of individuals with the optimal phenotype from the source. It is given by $r_D = m_D - r_{\max}$: note that r_D is thus positive when this optimal phenotype has negative growth rate (i.e. decays) in the sink.

Mutations. In the two environments, mutations occur at rate U and create independent and identically distributed (iid) random variations $\mathbf{dx}$ around the phenotype of the parent, for each trait. We assume here a standard $n-$dimensional isotropic Gaussian distribution of the mutation phenotypic effects, with mutational variance λ at each trait (Kimura, 1965; Lande, 1980). These assumptions induce a $1-$dimensional distribution of the mutation effects on fitness, given the relative fitness $m_p \leq 0$ of the

parent. This distribution, whose mean is $\mathbb{E}[s] = -n\ \lambda/2$, has already been described in Martin (2014) and is detailed in Appendix A.

Migration events. Migration sends randomly sampled individuals from the source into the sink, at rate $d > 0$ per unit time. Their relative fitness in the sink is $m_{migr}(\mathbf{x}) = -\|\mathbf{x}\|^2/2$, with $\mathbf{x}$ randomly sampled from the source's standing phenotype distribution.

2.3 Fitness distribution of the migrants

We assume that the distribution of phenotypes in the source is at mutation-selection balance. The resulting equilibrium distribution of phenotypes yields an equilibrium fitness distribution in the source. Under a weak selection strong mutation (WSSM) regime, this distribution is a negative gamma: (Martin and Roques, 2016, equation (10)): $m_{source} \sim -\Gamma(n/2, \mu)$, with $\mu := \sqrt{U\,\lambda}$. This WSSM regime can be quantitatively defined by the inequality $U > U_c := n^2\,\lambda/4$ (Martin and Roques, 2016, Appendix E).

To understand the dynamics of the fitness distribution in the sink, we need to compute the distribution of the relative fitness of the migrants m_{migr} when they arrive into the sink. To describe this distribution, we use its cumulant generating function: $\phi(z) := \ln\left(\mathbb{E}[e^{m_{migr}\,z}]\right)$, for any $z \geq 0$. Computations in Appendix B show that for any $z \geq 0$:

$$\phi(z) = -\frac{n}{2}\ln(1+\mu z) - m_D\,z + \frac{m_D\,\mu\,z^2}{1+\mu\,z}. \tag{3}$$

The corresponding distribution of m_{migr} is detailed in Appendix B and illustrated in Fig. 1. We observe that the mean absolute fitness of the migrants, which coincides with $\overline{r}(0) = \lim \overline{r}(t)$ as $t \to 0$, is given by

$$\overline{r}(0) = r_{\max} + \phi'(0) = r_{\max} - m_D - \mu\,n/2 = -r_D - \mu\,n/2, \tag{4}$$

with ϕ defined by (3). This initial growth rate is negative and corresponds to the decay rate (r_D) of the mean phenotype from the source (which is optimal there) plus a variance load ($\mu\,n/2$) due to the equilibrium variation around this mean.

2.4 Trajectories of fitness in the sink: a PDE approach

At time t, the population in the sink consists of the phenotypes $\{\mathbf{x}_i(t)\}_{i=1,\ldots,N(t)}$, with the corresponding values of relative fitnesses $\{m_i(t)\}_{i=1,\ldots,N(t)}$. In the absence of demography and immigration, the dynamics of the fitness distribution is traditionally investigated by a moment closure approximation (Burger, 1991; Gerrish and Sniegowski,

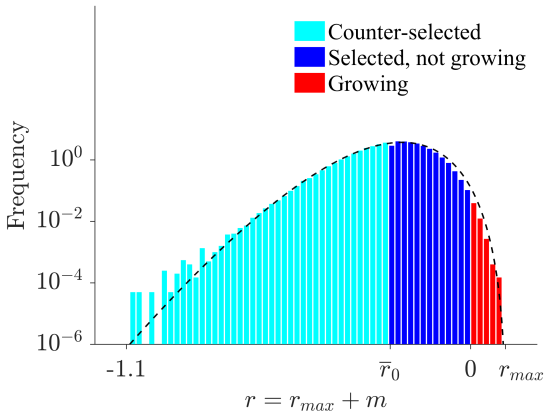

Figure 1: **Distribution of absolute fitness of the migrants in the sink.** The dashed line corresponds to the theoretical expected values of this distribution $p_{migr}(\cdot - r_{\max})$ (formula (A4) in Appendix B). The histogram corresponds to the distribution of migrants obtained in exact stochastic simulations after reaching the mutation-selection balance in the source (see Section 2.5). When the sink is empty, individuals are "counter-selected" if their fitness is below the mean fitness $\overline{r}(0)$ given by (4), "selected" if their fitness is above $\overline{r}(0)$, and "growing" if their fitness is positive. The parameter values are $r_{\max} = 0.1$, $U = 0.1$, $m_D = 0.3$, $\lambda = 1/300$, $n = 6$ and $N = 10^6$.

2012): the variations of the moment of order k depend on the moments of order larger than $(k+1)$ through a linear ordinary differential equation, and the resulting system is solved by assuming that the moments vanish for k larger than some value. A way around this issue is the use of cumulant generating functions (CGFs), which handle all moments in a single function. In a relatively wide class of evolutionary models of mutation and selection, the CGF of the fitness distribution satisfies a partial differential equation (PDE) that can be solved without requiring a moment closure approximation (Martin and Roques, 2016, Appendix B). We follow this approach here. The empirical CGF of the relative fitness in a population of $N(t)$ individuals with fitnesses $m_1(t), \ldots, m_{N(t)}(t)$ is defined by

$$C_t(z) = \ln\left(\frac{1}{N(t)}\sum_{i=1}^{N(t)} e^{m_i(t)\,z}\right), \tag{5}$$

for all $z \geq 0$. The mean fitness and the variance in fitness in the sink can readily be derived from derivatives, with respect to z, of the CGF, taken at $z = 0$: $\overline{m}(t) = \partial_z C_t(0)$ (and $\overline{r}(t) = r_{\max} + \partial_z C_t(0)$), and $V(t) = \partial_{zz} C_t(0)$ (the variance in fitness). In the absence of demography and immigration, and under a weak selection strong muta-

tion (WSSM) regime, (Martin and Roques, 2016, Appendix A) derived a deterministic nonlocal PDE for the dynamics of C_t. We extend this approach to take into account immigration effects and varying population sizes. This leads to the following PDE (derived in Appendix C):

$$\partial_t C_t(z) = \underbrace{\partial_z C_t(z) - \partial_z C_t(0)}_{selection} \; \underbrace{- \mu^2 \left(z^2 \, \partial_z C_t(z) + \frac{n}{2} z \right)}_{mutation} + \underbrace{\frac{d}{N(t)} \left(e^{\phi(z) - C_t(z)} - 1 \right)}_{migration,\ demography}, \; z \geq 0, \tag{6}$$

where we recall that $\mu := \sqrt{U\,\lambda}$. The immigration term depends on the relative fitness of the migrants, through $\phi(z)$, which is given by (3), and on $N(t)$, which satisfies the ODE (1), i.e. $N'(t) = (\partial_z C_t(0) + r_{\max})\, N(t) + d$. This leads to a well-posed coupled system (1) & (6) which can be solved explicitly, as shown in Appendix D.

The selection term in eq. (6) stems from the increase in frequency of each lineage proportionally to its Malthusian fitness (frequency-independent selection). The second term is the WSSM approximation ($U > U_c$) to a more complex term (Martin and Roques, 2016, Appendix A) describing the effect of mutation: it depends on the current background distribution (on $C_t(z)$) because of the fitness epistasis inherent in the FGM. The last term describes the effect of the inflow of migrants on lineage frequencies. It tends to equate $C_t(z)$ with $\phi(z)$, the CGF of fitnesses among migrants, proportionally to $d/N(t)$, the dilution factor of migrants into the current sink population.

2.5 Individual-based stochastic simulations

To check the validity of our approach, we used as a benchmark an individual-based, discrete time model of genetic drift, selection, mutation, reproduction and migration with non-overlapping generations.

Source population. A standard Wright-Fisher model with constant population size was used to compute the equilibrium distribution of phenotypes in the source. Our computations were carried out with $N^* = 10^6$ individuals in the source. Each individual $i = 1, \ldots, N^*$ has phenotype $\mathbf{x}_i \in \mathbb{R}^n$ and relative Malthusian fitness $m_i = -\|\mathbf{x}_i - \mathbf{x}^*\|^2/2$, with corresponding Darwinian fitness e^{m_i}. At each generation, N^* individuals are sampled with replacement proportionally to their Darwinian fitness. Mutations are simulated by randomly drawing, every generation and for each individual, a Poisson number of mutations, with rate U. Mutation acts additively on phenotype,

with individual effects $d\mathbf{x}$ drawn into an isotropic multivariate Gaussian distribution with variance λ per trait (see Section 2.2). Simulations were started with a homogeneous population ($\mathbf{x}_i = \mathbf{x}^*$ for all i at initial time) and ran for $20/\mu$ generations (the predicted time taken to reach a proportion q of the final equilibrium mean fitness is $\text{atanh}(q)/\mu$, see Appendix F, Section "Characteristic time" in Martin and Roques (2016); with $\text{atanh}(q) = 20$, one can consider that the equilibrium has been reached). An example of the distribution of absolute fitness in the resulting (equilibrium) source population, after migrating into the sink (distribution of $r_{\max} - \|\mathbf{x}_i\|^2/2$) is presented in Fig. 1.

Sink population. We started with $N(0) = 0$ individuals in the sink. Then, the process to go from generation t to generation $(t+1)$ is divided into three steps: (i) migration: a Poisson number of migrants, with rate d, was randomly sampled from the equilibrium source population, and added to the population in the sink; (ii) reproduction, selection and drift: each individual produced a Poisson number of offspring with rate $\exp(r_i) = \exp(r_{\max} + m_i)$ (absolute Darwinian fitness in the sink); (iii) mutation followed the same process as in the source population. The stopping criterion was reached when $N(t) > 1.5 \cdot 10^6$ individuals or $t > 5 \cdot 10^3$ to limit computation times.

All the Matlab® codes to generate individual-based simulations are provided in Supplementary File 1.

3 Results

3.1 Trajectories of mean fitness

Dynamics of $\overline{r}(t)$ and $N(t)$. The system (1) & (6) leads to an expression for the mean absolute fitness (Appendix D):

$$\overline{r}(t) = \frac{f(t) - 1}{\int_0^t f(\tau)\, d\tau}, \text{ with } f(t) = \exp\left[\left(r_{\max} - \mu\,\frac{n}{2}\right) t + \frac{m_D}{2\,\mu}(e^{-2\,\mu\,t} - 1)\right]. \qquad (7)$$

It also leads to an expression for the population size thanks to $N'(t) = \overline{r}(t)\, N(t) + d$. (see eq. (A7) in Appendix D).

As illustrated in Figs. 2-4, under the WSSM assumption ($U > U_c := n^2\,\lambda/4$), both the stochastic individual-based simulations and the analytic expressions show that sink invasion tends to follow four different phases, which are all the more pronounced as the

habitat difference m_D increases. Phase 1: During the first generations, the mean fitness slightly increases; Phase 2: The mean fitness remains stable. Phase 3: Rapid increase in mean fitness. Phase 4: The mean fitness stabilizes at some asymptotic value. In the case of establishment failure (Fig. 4), the adaptation process remains in Phase 2.

In Fig. 2, the trajectory from individual simulations (population's mean fitness, left panels and population size, right panels) is shown by colored lines, and the mean outcome over simulations is shown by dashed lines. This mean outcome over simulations can be compared to the deterministic theory in eq. 7. In all cases, the deviation between theory and mean of simulations is limited, but the stochastic variation around this mean can be substantial, as m_D increases. Further analysis of the deviation between theory and simulations is presented in Appendix E (exploring regimes outside the WSSM, when $U < U_c$), in Fig. 6 (over a wide range of parameters) and discussed in Appendix F.

Phenotypic dynamics over the different phases of invasion. Obviously the division into four phases could be deemed somewhat arbitrary, and it is clearly less marked with milder habitat difference (top panels of Fig. 2). However, it does convey the qualitative chronology of the whole process in all cases. This can be further understood by exploring the dynamics of the phenotypic distribution over time: a typical example for a single simulation is given in Fig. 3, at four times corresponding to each of the four phases. We show here the marginal phenotypic distribution along the one meaningful dimension, that for which the optimum is shifted between source and sink (the optimum in the sink is 0, and the optimum in the source $\mathbf{x}^* = (\sqrt{2\,m_D}, 0, \ldots, 0)$). The corresponding trajectories of fitness and population size are available in Appendix G (Fig. A2). A video file of the phenotype distribution is also available as Supplementary File 2.

During Phases 1 and 2, the phenotypic distribution is fairly stable and slightly shifted from the source distribution towards the sink optimum. The short Phase 1 merely witnesses an increase in population size from zero to the semi-stable Phase 2. We suggest that this semi-stable state approximately corresponds to a macroscopic "equilibrium" between migration and selection on the bulk of phenotypes. Here, we conjecture a negligible impact of mutation on this bulk because simulations in the absence of mutation in the sink yield a very similar phenotypic distribution during Phase 2 (Appendix L, Fig. A6). However, over the course of Phase 2, a second mode slowly appears closer to the sink optimum, due to the invasion of rare, better adapted, phenotypes (generated by the combined effects of rare adapted migrants and *de novo* mutation in the sink).

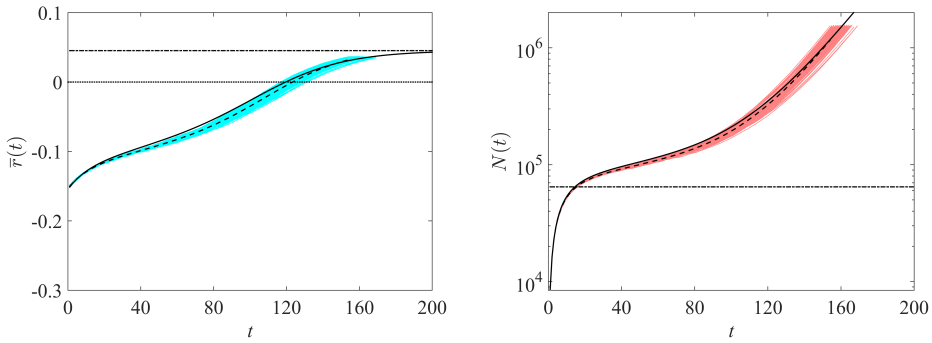

(a) $m_D = 0.2$ (b) $m_D = 0.2$

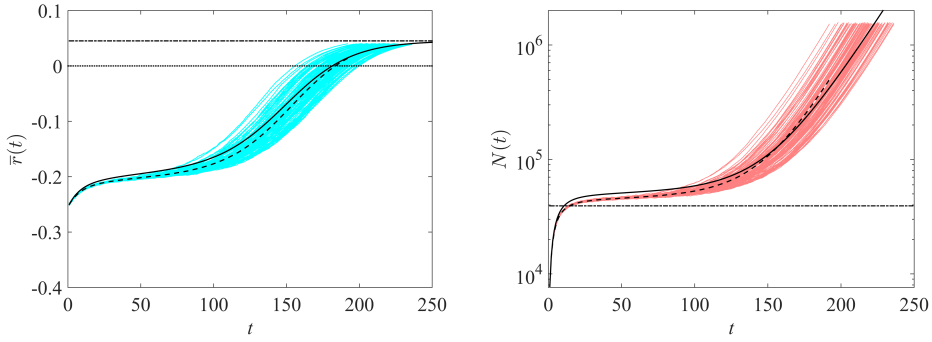

(c) $m_D = 0.3$ (d) $m_D = 0.3$

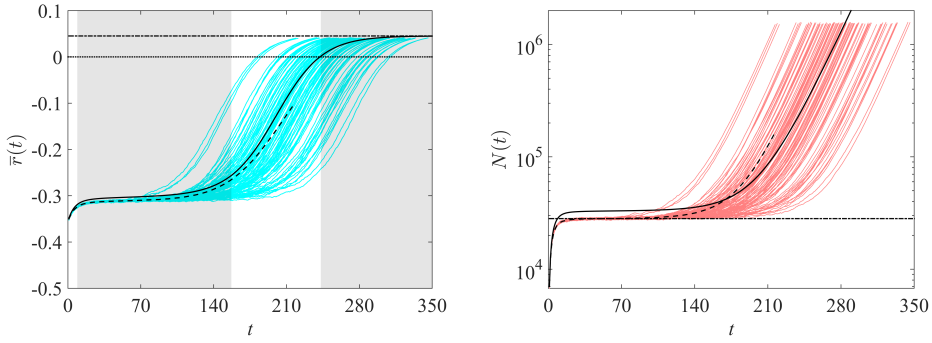

(e) $m_D = 0.4$ (f) $m_D = 0.4$

Figure 2: **Trajectories of mean fitnesses and population sizes in a WSSM regime, depending on the habitat difference.** Solid lines: analytical predictions given by formulae (1) and (7) vs 100 trajectories obtained by individual-based simulations (blue curves for $\overline{r}(t)$ and red curves for $N(t)$; dashed lines: mean values averaged over the 100 populations). Horizontal dashed-dotted lines: theoretical value of $\overline{r}(\infty) = r_{\max} - \mu\, n/2$ (left panels) and equilibrium population size $-d/\overline{r}(0)$ in the absence of adaptation (right panels). The four phases of invasion (Phases 1-4, see main text) are illustrated by distinct shaded areas on panel (e). The parameter values are $U = 0.1$ (thus, $U > U_c = 0.03$, which is consistent with the WSSM regime), $r_{\max} = 0.1$, $\lambda = 1/300$, $n = 6$ and $d = 10^4$. Due to the stopping criterion $N(t) = 1.5 \cdot 10^6$ was reached, the mean values could not be computed over the full time span.

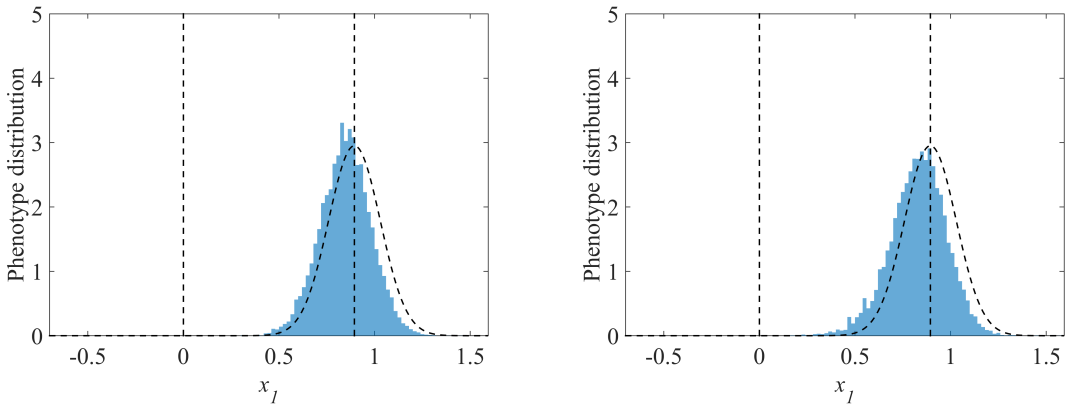

(a) Phase 1: $t = 10$

(b) Phase 2: $t = 60$

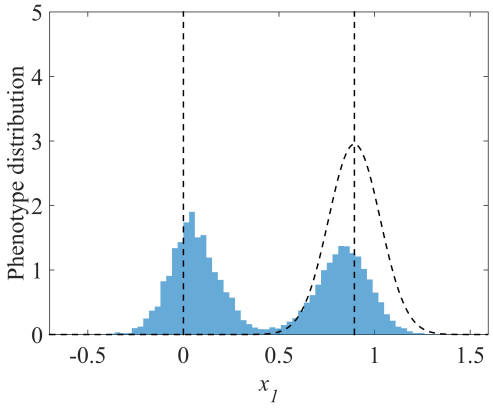

(c) Phase 3: $t = 220$

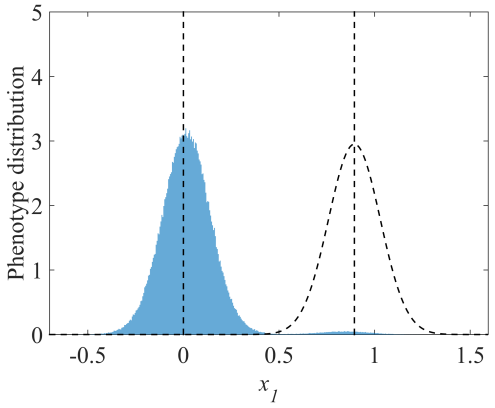

(d) Phase 4: $t = 300$

Figure 3: **Marginal phenotype distribution in the sink, along the direction x_1.** The vertical dotted lines correspond to the sink ($x_1 = 0$) and source ($x_1 = \sqrt{2\,m_D}$) optima. The black dotted curve corresponds to the theoretical distribution of migrant's phenotypes in the sink (Gaussian distribution, centered at $x_1 = \sqrt{2\,m_D}$, and with variance $\mu = \sqrt{U\,\lambda}$). In all cases, the parameter values are $m_D = 0.4$, $U = 0.1$, $r_{\max} = 0.1$, $\lambda = 1/300$, $n = 6$ and $d = 10^4$.

When the second mode generated during Phase 2 becomes significant in frequency, Phase 3 starts with a rapid increase of the second mode (and of mean fitness), because phenotypic and fitness variance are then maximized. The last Phase 4 corresponds to the new equilibrium dominated by a mutation selection balance around the sink optimum. In the present model without density limitations, migration becomes ultimately negligible as the sink population explodes, and its phenotypic distribution ultimately reaches exactly a new mutation-selection balance.

Sources of the stochastic deviations around the deterministic theory. In Fig. 2, most of the stochastic deviations from the mean trajectory (dashed line) or model's prediction (plain lines) appears to arise during Phase 2. Indeed, after this phase, the trajectories appear regular, similar in shape with the deterministic model, but *shifted in time* relative to this expected trajectory. This suggests that after phase 2, the system is roughly deterministic, with a waiting time that is stochastic, determined during Phase 2. Intuitively, this stochastic variability in the duration of Phase 2 should depend on the population size at this stage. Let us approach this population size by the equilibrium size without evolution, see Appendix F: $d/|\overline{r}(0)| = d/|m_D + \mu\, n/2 - r_{\max}|$. We observe that it decreases as m_D is increased, leading to more variation in the waiting time before Phase 3, as observed in the simulations of Fig. 2.

However, quantitatively, a fairly limited variation of m_D (only by a factor 2 from Fig. 2 (a,b) to (e,f)) implies a large increase in the stochastic variation of the waiting time. This suggests that the effect does not only lie in a mere population size effect but also in the fact that, as m_D increases, the proportion of mutant genotypes resistant to the sink (coming from the source or arising *de novo*) drops very sharply with maladaptation (Anciaux et al., 2019). By "resistant to the sink", we mean a genotype with a positive growth rate in that environment (in the absence of migration). The sink population ultimately descends from these few resistant lineages, which arise at variable times and show stochasticity in their early growth. These two eects make the initial dynamics stochastic; only when the lineage has grown in number the dynamics become deterministic. At large m_D, a few resistant lineages determine ultimate trajectory of the entire sink population, hence there is more variability across replicates.

Effect of the immigration rate. The value of $\overline{r}(t)$ in formula (7) does not depend on the immigration rate d. Thus, only the population size dynamics are influenced by the immigration rate, but not the evolutionary dynamics. Actually, a simple mathematical argument (Appendix H) shows that this property will apply beyond the present model. The result arises for any model where (i) the evolutionary and demographic dynamics in the sink are density-independent (apart from the impact of migration) and (ii) the sink is initially empty (or at least $d \gg N(0)$). This means that it should apply for a broad class of models of asexual evolution in black-hole sinks. Whether it applies outside of this class of models remains an open question (e.g. how sexual reproduction would affect the result).

An intuition for the independence of $\overline{r}(t)$ on d might be framed as follows: if d is increased (resp. decreased), the sink fills in more (resp. less) rapidly, from $N(0) = 0$,

proportionally to the increase (resp. decrease) in d, at all times. Therefore things cancel out in the migration contribution on frequencies ($d/N(t)$ is unaffected), and this contribution is the only one where d enters the dynamics. Overall increasing or decreasing d thus has no effect on genotype frequency dynamics, although it does affect population sizes.

Long time behavior. As seen in Fig. 2, $\overline{r}(t)$ converges towards an asymptotic value $\overline{r}(\infty)$ at large times. The expression (7) shows that this value depends on $r_{\max}$, μ and n. It becomes dependent on the habitat difference m_D, only in the case of establishment failure. More precisely, we get:

$$\begin{aligned} &\text{if } r_{\max} - \mu\, n/2 \geq 0 \text{ then } \overline{r}(\infty) = r_{\max} - \mu\, n/2, \text{ and } N(\infty) = \infty \\ &\text{if } r_{\max} - \mu\, n/2 < 0 \text{ then } \overline{r}(\infty) = r_{\max} - \mu\, n/2 - \delta(m_D), \text{ and } N(\infty) = -d/\overline{r}(\infty), \end{aligned} \tag{8}$$

for some function $\delta(m_D)$ such that $m_D > \delta(m_D) > m_D/8$ for μ large enough (the inequality $\delta(m_D) > m_D/8$ is true whatever the phenotype dimension n). When n is large enough, sharper lower bounds can be obtained, e.g. $\delta(m_D) > 3\, m_D/8$ for $n \geq 6$), see Appendix I.

These asymptotic results can be interpreted as follows. Below some threshold ($U < U_{lethal} := 4r_{\max}^2/(\lambda\, n^2)$, or equivalently $\mu < \mu_{lethal} := 2r_{\max}/n$), establishment is always successful and the sink population ultimately explodes (as we ignore density-dependence in the sink). As $d/N(\infty) = 0$, the demographic and evolutionary effects of migrants thus become negligible (being diluted in an effectively infinite population). The sink population thus reaches mutation-selection balance, with a mutation load $\mu\, n/2$, as if it was isolated. It ultimately grows exponentially at rate $r_{\max} - \mu\, n/2$ as illustrated in Fig. 2.

On the contrary, large mutation rates ($U \geq U_{lethal}$ or equivalently $\mu \geq \mu_{lethal}$) lead to establishment failure, which is a form of lethal mutagenesis (see Bull et al. (2007) for viruses and Bull and Wilke (2008) for bacteria) illustrated in Fig. 4. In this regime, the mutation load $\mu\, n/2$ is larger than the absolute maximal fitness $r_{\max}$ in the sink. Therefore, at mutation-selection balance and even in the absence of any migration, the population could never show positive growth: establishment is impossible because the fitness peak is too low, given the mutation rate and effect. We further identify a "jump" of amplitude $\delta(m_D)$ in the equilibrium mean fitness, as μ increases beyond the lethal mutagenesis threshold (illustrated in Fig. 5). Then, the population ultimately reaches a stable size determined by an immigration - decay equilibrium: a migration load can build up at equilibrium ($\delta(m_D)$) together with the mutation load ($\mu\, n/2$). This

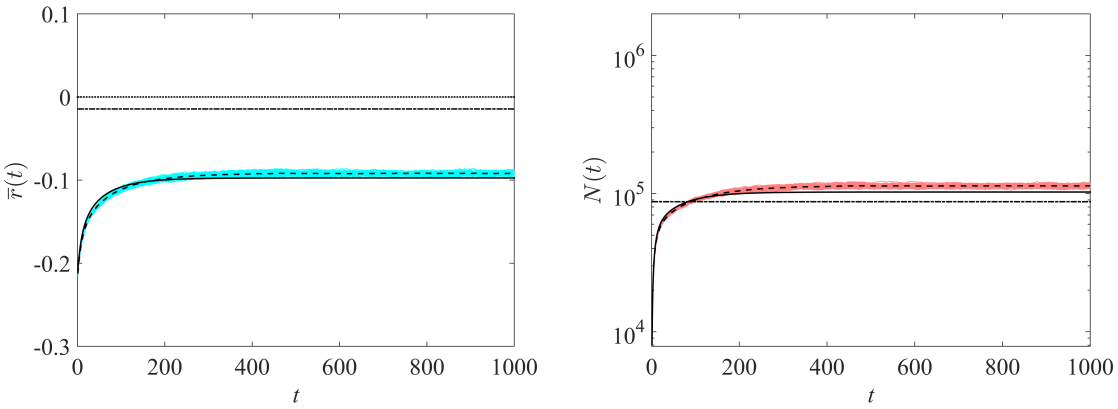

(a) $U = 0.44 > U_{lethal}$ (b) $U = 0.44 > U_{lethal}$

Figure 4: **Trajectories of mean fitnesses and population sizes, lethal mutagenesis regime.** Same line types as in Fig. 2. Other parameter values are $m_D = 0.2$, $r_{\max} = 0.1$, $\lambda = 1/300$, $n = 6$ and $d = 10^4$, leading to a theoretical threshold value for lethal mutagenesis $U_{lethal} = 4r_{\max}^2/(\lambda\, n^2) = 0.33$. The panel (a) illustrates the change in the behavior of the equilibrium mean fitness as $r_{\max} - \mu\, n/2$ becomes negative.

migration load is produced by the constant inflow of maladapted genotypes from the source and does depend on the habitat difference m_D. It is this migration load that creates the "phase transition" in equilibrium fitness as μ crosses beyond μ_{lethal}, the lethal mutagenesis threshold (Fig. 5).

3.2 Establishment time t_0

Of critical importance is the waiting time until the sink becomes a source, when this happens, namely the time t_0 at which $\overline{r}(t)$ becomes positive. This section is devoted to the analysis of this time.

Derivation of an analytical expression. Using expression (7), we can solve the equation $\overline{r}(t_0) = 0$. We recall that, due to our assumptions, $t_0 > 0$, i.e. $\overline{r}(0) = r_{\max} - \mu\, n/2 - m_D < 0$.

The result in (8) shows that $t_0 = \infty$ if $r_{\max} - \mu\, n/2 \leq 0$ (establishment failure). In the case of successful establishment ($m_D > \overline{r}(\infty) = r_{\max} - \mu\, n/2 > 0$), the waiting time to this establishment is:

$$t_0 = \frac{1}{2\mu}\left[c + W_0\left(-c\, e^{-c}\right)\right],\ c = \frac{m_D}{r_{\max} - \mu\, n/2}, \tag{9}$$

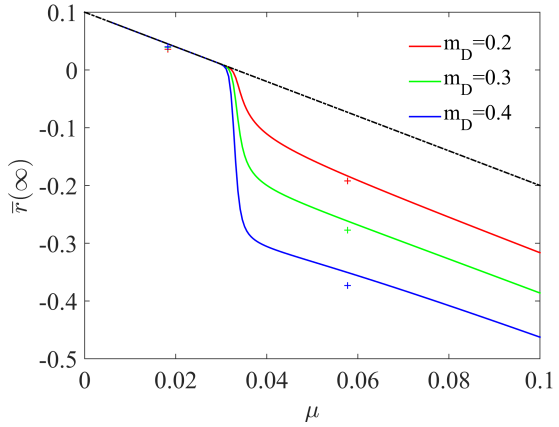

Figure 5: **Mean fitness at large times, dependence with μ and m_D.** The solid lines are the values given by formula (8). The crosses correspond to the result of individual-based simulations. The dashed-dot line corresponds to $r_{\max} - \mu\, n/2$; the gap between the dashed-dot line and the solid lines represents the amplitude of the jump $\delta(m_D)$. Parameter values: $r_{\max} = 0.1$, $n = 6$.

with W_0 the principal branch of the Lambert-W function (see Appendix J).

First of all, eq. (9) shows that the waiting time is independent of the dispersal rate d. This was further supported by individual-based simulations (Fig. 6a) as t_0 was found to drop rapidly to its predicted value as d increases, to then become independent of d. The waiting time satisfies $(c-1)/(2\,\mu) \leq t_0 \leq (c-1)/\mu$ for all $c \geq 1$. As c becomes larger, $W_0\left(-c\,e^{-c}\right) \approx 0$, and $t_0 \approx c/(2\,\mu)$, so the establishment time increases close to linearly with the habitat difference m_D. The condition $c \geq 1$ corresponds to $m_D \geq r_{max} - \mu\, n/2 \approx 0.05$ in Fig. 6c (lower values of m_D lead to $t_0 = 0$ and are therefore not taken into account). This near-linear dependence was also found in the individual-based simulations, at least until the habitat difference becomes too large, compared to mutation and migration. In that case, the sink population remains fairly small for a long time and our deterministic approximation no longer applies, at least in the early phases (1 and 2) of invasion (see Appendix F). Eq. (9) also implies that the establishment time t_0 decreases with $r_{\max}$ and increases with n. The dependence with respect to the mutational parameter μ is more subtle: as μ is increased, $t_0(\mu)$ first decreases until μ reaches an "optimal value" (minimizing invasion time), then $t_0(\mu)$ increases until μ reaches the lethal mutagenesis threshold ($\mu_{lethal} = 2\ r_{\max}/n$). This behaviour always holds, as proven analytically in Appendix J. This non-monotonic variation of t_0 with mutation rate (here with $\mu = \sqrt{U\lambda}$) was also found in individual-based simulations (Fig. 6b). Fig. A4 in Appendix L shows that local mutation in the

sink can either reduce or increase t_0 depending on μ and m_D.

Effect of an intermediate sink. The simulations identify a sharp transition, in the habitat difference, beyond which establishment does not occur (or occurs at very large times), see Appendix K. We see in Fig. 6 that as m_D gets close to this threshold, the dependence between t_0 and m_D shifts from linear to superlinear (convex). Based on previous results on evolutionary rescue in the FGM (Anciaux et al., 2018), we conjecture that this pattern is inherent to the phenotype fitness landscape model. In the FGM, higher habitat difference m_D is caused by a larger shift in optimum from source to sink. This has two effects, (i) a demographic effect (faster decay of new migrants, on average) and (ii) an evolutionary effect. This latter effect is simply due to the geometry of the landscape. Indeed, when the shift in optimum from source to sink is larger, there are fewer genotypes, in the migrant pool, that can grow in the sink and they tend to grow more slowly. This effect is highly nonlinear with m_D, showing a sharp transition in the proportion of resistant genotypes beyond some threshold (for more details see Anciaux et al., 2018).

We argue that this type of dependence has important implications for the potential effect of an intermediate milder sink, with phenotype optimum $\mathbf{x}^I$ in between $\mathbf{x}^*$ (optimum in the source) and 0 (optimum in the sink), connected by a stepping-stone model of migration. A natural question is then whether the presence of this intermediate sink affects the waiting time to establish in the harsher sink. In that respect, assume that the overall habitat difference (fitness distance between optima) is the same with and without the intermediate habitat I: schematically, $m_D = m_D(\mathbf{x}^* \to 0) = m_D(\mathbf{x}^* \to \mathbf{x}^I) + m_D(\mathbf{x}^I \to 0)$. When m_D is low, t_0 is roughly linear with m_D so that it may take a similar time to establish in two step and in one (the sum of intermediate establishment times would be the same as that to establish in a single jump). However, for higher habitat difference where t_0 is superlinear with m_D, the intermediate habitat could provide a springboard to invade the final sink, if both intermediate jumps are much faster than the leap from source to final sink.

To check this theory, we considered a new individual-based model with an intermediate habitat with phenotype optimum $\mathbf{x}^I$ such that $\|\mathbf{x}^* - \mathbf{x}^I\|^2/2 = \|\mathbf{x}^I\|^2/2 = m_D/2$. The dynamics between the source and the sink are the same as those described in Section 2.5. In addition, we assume that (1) the source also sends migrants to the intermediate habitat at a rate d; (2) reproduction, selection and drift occur in the intermediate habitat following the same rules as in the sink, until the population $N_I(t)$ in the intermediate habitat reaches the carrying capacity $K = N^*$ (same population

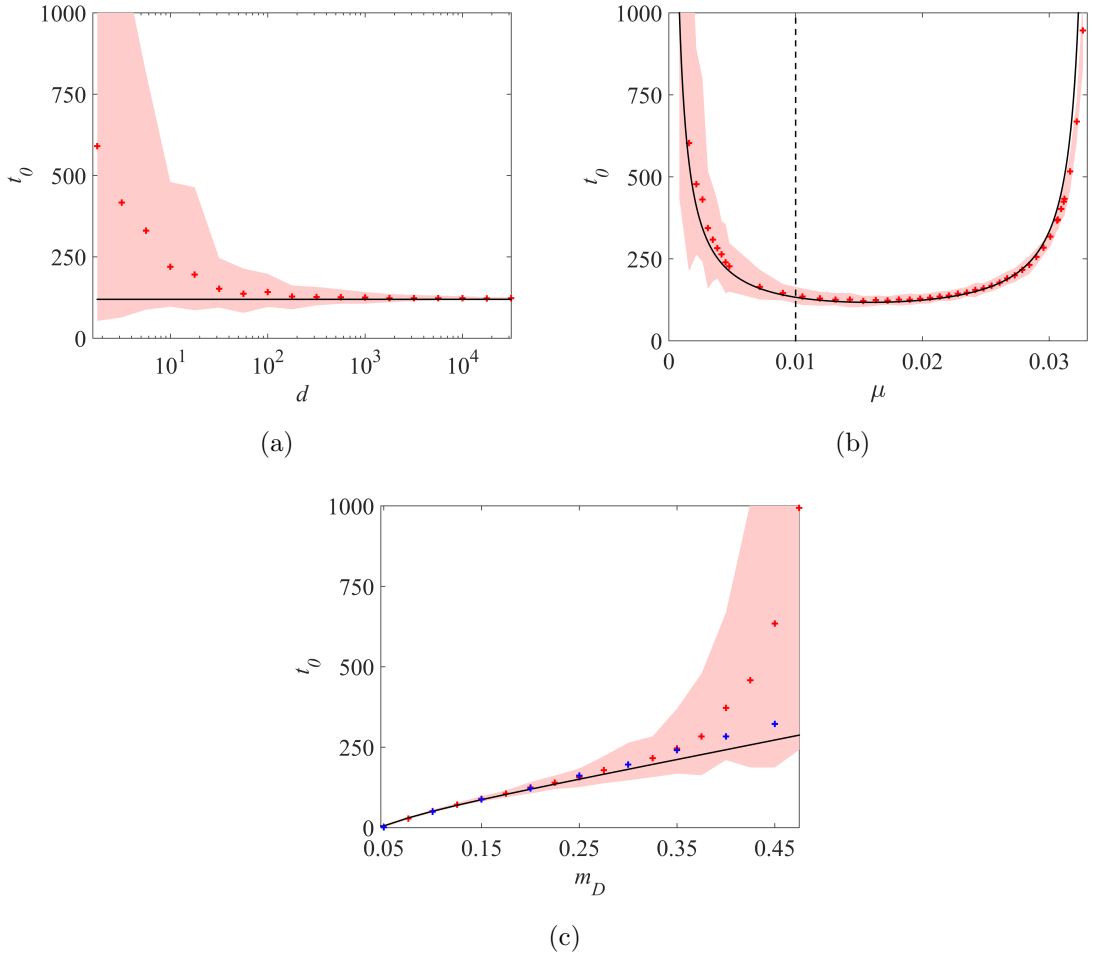

Figure 6: **Establishment time t_0, dependence with the immigration rate d, the mutational parameter μ and the habitat difference m_D.** Theoretical value of t_0 (black curve) vs value obtained with individual-based simulations (red crosses) and interval between the 0.025 and 0.975 quantiles of the distribution of t_0 obtained from 10^3 simulations (pink shading), with fixed $m_D = 0.2$, $U = 0.1$ (panel a), $m_D = 0.2$, $d = 10^3$ (panel b) and fixed $d = 10^3$, $U = 0.1$ (panel c). The vertical dotted line in panel b corresponds to $U = U_c$ ($\mu = \sqrt{U_c\,\lambda}$). The blue crosses in panel (c) correspond to the establishment time $t_0^I(m_D)$, obtained by individual-based simulations, in the presence of an intermediate habitat with phenotype optimum $\mathbf{x}^I$ such that $\|\mathbf{x}^* - \mathbf{x}^I\|^2/2 = \|\mathbf{x}^I\|^2/2 = m_D/2$. In all cases, the parameter values are $r_{\max} = 0.1$, $\lambda = 1/300$, $n = 6$.

size as in the source); (3) the intermediate habitat sends migrants to the ultimate sink, at rate $d\,N_I(t)/N^*$. Then, we computed the time $t_0^I(m_D)$ needed to establish in the final sink, in the presence of the intermediate habitat (value averaged over 100 replicate simulations).

The results presented in Fig. 6c (blue crosses) confirm that for small m_D, the presence of an intermediate habitat has almost no effect ($t_0^I(m_D) \approx t_0(m_D)$). However, when m_D becomes larger and $t_0(m_D)$ becomes superlinear, the establishment time in the sink is dramatically reduced by the presence of the intermediate sink ($t_0^I(m_D) \ll t_0(m_D)$; e.g., for $m_D = 0.5$, $5 \cdot 10^3 \approx t_0(m_D) \gg t_0^I(m_D) \approx 364$).

4 Discussion

We derived an analytically tractable PDE-ODE framework describing evolutionary and demographic dynamics of asexuals in a source-sink system. This approach reveals the typical shape of the trajectories of mean fitness and population sizes in a sink: (1) in the case of establishment failure, after a brief increase, the mean fitness remains stable at some negative level which depends on the habitat difference; (2) in the case of successful establishment, this "plateau" is followed by a sudden increase in mean fitness up to the point where it becomes positive and the sink becomes a source. Note that here, we ignored density dependent effects in the sink, so that mean fitness ultimately converges towards an equilibrium that is independent of any migration effect, the latter being diluted into an exploding population.

The first three phases predicted by the model, for the case of successful establishment, are qualitatively observed in (Dennehy et al., 2010), an experimental study of invasion of a black-hole sink (an asexual bacteriophage shifting to a new bacterial host). The "host shift" scenario in their Fig. 3 corresponds roughly to our scenario with a population evolved on the native host sending migrants to a new host. The conditions may differ however as the population may not be initially at equilibrium in the native host at the onset of migration. Yet, the dynamics are qualitatively similar to those in our Fig. 2, although the time resolution in the data is too limited to claim or test any quantitative agreement. An extension of the present work could be to allow for non-equilibrium source populations, which can readily be handled by the PDE (6) (reformulating $\phi(z) = \phi(z,t)$). However, our analytical result on t_0 does rely on an equilibrium source population. Note also that the four phases identified here are observed, in simulations, even in the low d or low U regimes where our analytical derivations can break down quantitatively. Therefore, while the model may provide

qualitatively robust insight, quantitative analyses are necessary to really test its predictions. This would ideally include associated measures of decay rates r_D, mutation rate U and ideally maximal possible growth rate $r_{\max}$, with a known immigration rate d.

Quite unexpectedly, the evolutionary dynamics (especially the waiting time t_0 to establishment) do not depend on the immigration rate. This emerges mathematically from the fact that the evolutionary dynamics only depend on the population size through the ratio $N(t)/d$ between the current population size and the immigration rate, this ratio itself remaining independent of d. This is confirmed by stochastic individual-based simulations (Fig. 6a): establishment time roughly decreases as $1/d$ when d is small but indeed stabilizes as d becomes larger. This result *a priori* extends to any model where evolution and demography are density-independent (see Appendix F). However density dependent effects on demography or evolution (including sexual reproduction) might alter this outcome. Yet, we argue that purely demographic effects due to a finite carrying capacity in the sink environment should have limited impact on the conclusions of our model, up until establishment time (as long as K is large enough).

Instead of the establishment time t_0, one may adopt an "evolutionary rescue" viewpoint, and focus on the time t_1 at which a lineage *ultimately* destined to produce a resistant genotype, enters the sink. This lineage may be very rare by $t = t_1$, it may even not be resistant itself but only destined to produce a mutant offspring that will be. The time t_0 at which the sink will *de facto* be a positively growing source can thus be far later. A study and comparison of both waiting times is interesting and feasible, but beyond the scope of the present paper. This remark, however, has one key implication: migration may be stopped long before t_0 and the sink may still ultimately become a source, with some probability that depends on d.

Some insight into the possible effects of management strategies, e.g. quarantine (d), lethal mutagenesis (U), prophylaxis (m_D and $r_{\max}$), can be developed from the results presented here.

Migration (propagule pressure) is considered an important determinant of the success of biological invasions in ecology (Von Holle and Simberloff, 2005; Lockwood et al., 2005). Consistently, it has been shown that the factors increasing potential contacts between human populations and an established animal pathogen or its host tend to increase the risk of emergence of infectious diseases (Morse, 2001). Under the "repeated rescue approach" above, it is indeed expected that emergence risk should increase with the contact rate. However, the present work shows that the time at which this emer-

gence will be *de facto* effective (visible) may be unaffected by this contact rate. This means that care must be taken in the criteria chosen to evaluate strategies, and between the minimization of emergence risk *vs.* emergence time.

The use of a chemical mutagen to avoid the adaptation of a microbial pathogen and the breakdown of drugs is grounded in lethal mutagenesis theory (Bull et al., 2007; Bull and Wilke, 2008). Our approach successfully captures the occurrence of this phenomenon: the establishment fails when the mutation rate U exceeds a certain threshold, which depends on $r_{\max}$, on the mutational variance λ and on the dimension of the phenotypic space. Additionally, once this threshold is reached, the equilibrium mean fitness ceases to depend linearly on the mutational parameter ($\mu = \sqrt{U\,\lambda}$), but rapidly decays (see Fig. 5). The existence of this negative "jump" in the equilibrium mean fitness, whose magnitude depends on the habitat difference, leaves no room for evolutionary rescue. Conversely, our approach also reveals that below the lethal mutagenesis threshold, increasing the mutation rate decreases the establishment time as $1/\sqrt{U}$. Hence, the use of a mutagen may be a double-edged sword since it can both hamper or increase the potential for adaptation in the sink. Note that these effects of lethal mutagenesis are only meaningful when the maximum absolute fitness in the source is larger than that in the sink ($r_{\max}$); otherwise, the source itself would be destroyed by lethal mutagenesis.

As expected, the establishment time t_0 increases with the habitat difference m_D; the population simply needs more time to adapt to harsher environmental conditions. Increasing m_D or decreasing $r_{\max}$, whenever possible, are probably the safest ways to reduce the risks of biological invasions through adaptive processes or cross-species transmissions of pathogens (in both low and high d regimes). The precise dependence of t_0 with respect to m_D brings us further valuable information. As long as our approach is valid (not too large m_D, leading to finite establishment times), a linear dependence emerges. It suggests that, in a more complex environment with a source and several neighbouring sinks connected by a stepping stone model of migration, the exact pathway before establishment occurs in a given sink does not really matter. Only the sum of the habitat differences due to habitat shifts has an effect on the overall time needed to establish in the whole system. Conversely, for larger m_D our analytical approach is not valid, and the numerical simulations indicate a convex (superlinear) dependence of t_0 with respect to m_D. In such case, for a fixed value of the cumulated habitat difference, the establishment time in the sink could be drastically reduced by the presence of intermediate sink habitats.

This result, which needs to be confirmed by more realistic modelling approaches and empirical testing, might have applications in understanding the role of so-called

"preadaptation" in biological invasions. Recent adaptation to one or more facets of the environment within the native range has been proposed as a factor facilitating invasions to similar environments (e.g. Hufbauer et al., 2012, anthropogenically induced adaptation to invade). Our results suggest that preadaptation might reduce the overall time to invasion (i.e., taking the preadapation period into account) only when invading habitats very different from the native habitat (as measured by the habitat difference).

The effect of a given environmental challenge, and thus their joint effects when combined (Rex Consortium, 2013), might be modelled in various ways in a fitness landscape framework (see also discussions in Harmand et al., 2017; Anciaux et al., 2018). The first natural option is to consider that multiple stresses tend to pull the optimum further away, and possibly lower the fitness peak $r_{\max}$. In the simplified isotropic model studied here, a larger shift in optimum amounts to increasing m_D. However, a possibly more realistic anisotropic version, with some directions favored by mutation or selection, might lead to directional effects (where two optima at the same distance are not equally easy to reach) and be particularly relevant to multiple stress scenarios. Such a more complex model could be handled by focusing on a single dominant direction (discussed in Anciaux et al., 2018), or by following multiple fitness components (one per direction). With this last approach, (Hamel et al., 2019) showed that, in a single-population model without immigration and demography, most of the mathematical results in (Martin and Roques, 2016) in the WSSM regime can be extended to take anisotropic effects into account (e.g., on mutations). This leads to trajectories of adaptation which can exhibit several "plateaus", corresponding to successive adaptation along each direction, at time scales which depend on the respective mutational variances at each trait. The joint effects of immigration and anisotropy could be handled by combining their results with the framework developed here. Although some of the effects predicted in the present work should still hold within this more general framework (for instance regarding the effect of d and m_D), the four-phases trajectory of adaptation may be modified (occurrence of additional plateaus?), and the mutational effects on the establishment time should depend on the directions favored by mutation.

Acknowledgments

This work was supported by the French Ministry of Higher Education, Research and Innovation (MESRI allocation doctorale to Y.A.), and the French Agence Nationale de la Recherche (ANR-13-ADAP-0016 "Silentadapt" to G.M., ANR-13-ADAP-0006 "MeCC" and ANR-14-CE25-0013 "NONLOCAL" to L.R. and ANR-18-CE45-0019 "RESISTE"

to G.M., J.P. and L.R.). This work was fostered by stimulating discussions with Ophélie Ronce and François Hamel. The authors have no conflict of interest to declare.

References

Alexander, H. K., G. Martin, O. Y. Martin, and S. Bonhoeffer (2014). Evolutionary rescue: linking theory for conservation and medicine. Evolutionary applications 7(10), 1161–1179.

Anciaux, Y., L.-M. Chevin, O. Ronce, and G. Martin (2018). Evolutionary rescue over a fitness landscape. Genetics 209, 265–279.

Anciaux, Y., A. Lambert, O. Ronce, L. Roques, and G. Martin (2019). Population persistence under high mutation rate: from evolutionary rescue to lethal mutagenesis. Evolution.

Barton, N. and A. Etheridge (2017). Establishment in a new habitat by polygenic adaptation. Theoretical Population Biology 122, 110–127.

Blackburn, T. M., P. Pyšek, S. Bacher, J. T. Carlton, R. P. Duncan, V. Jarošík, J. R. Wilson, and D. M. Richardson (2011). A proposed unified framework for biological invasions. Trends in Ecology & Evolution 26(7), 333–339.

Bull, J. J., R. Sanjuan, and C. O. Wilke (2007). Theory of lethal mutagenesis for viruses. Journal of Virology 81(6), 2930–2939.

Bull, J. J. and C. O. Wilke (2008). Lethal mutagenesis of bacteria. Genetics 180(2), 1061–1070.

Burger, R. (1991). Moments, cumulants, and polygenic dynamics. Journal of Mathematical Biology 30(2), 199–213.

Colautti, R. I., J. M. Alexander, K. M. Dlugosch, S. R. Keller, and S. E. Sultan (2017). Invasions and extinctions through the looking glass of evolutionary ecology. Philosophical Transactions of the Royal Society B: Biological Sciences 372(1712), 20160031.

Débarre, F., O. Ronce, and S. Gandon (2013). Quantifying the effects of migration and mutation on adaptation and demography in spatially heterogeneous environments. Journal of Evolutionary Biology 26(6), 1185–1202.

Dennehy, J. J., N. A. Friedenberg, R. C. McBride, R. D. Holt, and P. E. Turner (2010). Experimental evidence that source genetic variation drives pathogen emergence. Proceedings of the Royal Society B: Biological Sciences 277(1697), 3113–3121.

Drury, K. L. S., J. M. Drake, D. M. Lodge, and G. Dwyer (2007). Immigration events dispersed in space and time: Factors affecting invasion success. Ecological Modelling 206, 63–78.

Furrer, R. D. and G. Pasinelli (2016). Empirical evidence for source–sink populations: a review on occurrence, assessments and implications. Biological Reviews 91(3), 782–795.

Garnier, J., L. Roques, and F. Hamel (2012). Success rate of a biological invasion in terms of the spatial distribution of the founding population. Bulletin of Mathematical Biology 74, 453–473.

Gerrish, P. J. and P. D. Sniegowski (2012). Real time forecasting of near-future evolution. Journal of the Royal Society Interface 9(74), 2268–2278.

Gomulkiewicz, R., R. D. Holt, and M. Barfield (1999). The effects of density dependence and immigration on local adaptation and niche evolution in a black-hole sink environment. Theoretical Population Biology 55(3), 283–296.

Gomulkiewicz, R., R. D. Holt, M. Barfield, and S. L. Nuismer (2010). Genetics, adaptation, and invasion in harsh environments. Evolutionary Applications 3(2), 97–108.

Hamel, F., F. Lavigne, G. Martin, and L. Roques (2019). Dynamics of adaptation in an anisotropic phenotype-fitness landscape. bioRxiv.

Harmand, N., R. Gallet, R. Jabbour-Zahab, G. Martin, and T. Lenormand (2017). Fisher's geometrical model and the mutational patterns of antibiotic resistance across dose gradients. Evolution 71(1), 23–37.

Holt, R. D. (2009). Bringing the Hutchinsonian niche into the 21st century: ecological and evolutionary perspectives. Proceedings of the National Academy of Sciences 106(Supplement 2), 19659–19665.

Holt, R. D., M. Barfield, and R. Gomulkiewicz (2004). Temporal variation can facilitate niche evolution in harsh sink environments. The American Naturalist 164(2), 187–200.

Holt, R. D., M. Barfield, and R. Gomulkiewicz (2005). Theories of niche conservatism and evolution: could exotic species be potential tests, pp. 259–290. Sinauer Associates Sunderland, MA.

Holt, R. D., R. Gomulkiewicz, and M. Barfield (2003). The phenomenology of niche evolution via quantitative traits in a "black-hole" sink. Proceedings of the Royal Society of London B: Biological Sciences 270(1511), 215–224.

Hufbauer, R. A., R. Facon, V. Ravigné, J. Turgeon, J. Foucaud, C. E. Lee, O. Rey, and A. Estoup (2012). Anthropogenically induced adaptation to invade (AIAI): contemporary adaptation to human-altered habitats within the native range can promote invasions. Evolutionary Applications 5(1), 89–101.

Jansen, M., A. Coors, R. Stoks, and L. De Meester (2011). Evolutionary ecotoxicology of pesticide resistance: a case study in Daphnia. Ecotoxicology 20(3), 543–551.

Kimura, M. (1965). A stochastic model concerning the maintenance of genetic variability in quantitative characters. Proceedings of the National Academy of Sciences 54(3), 731–736.

Kirkpatrick, M. and N. H. Barton (1997). Evolution of a species'range. The American Naturalist 150, 1–23.

Lande, R. (1980). The genetic covariance between characters maintained by pleiotropic mutations. Genetics 94(1), 203–215.

Lenormand, T. (2002). Gene flow and the limits to natural selection. Trends in Ecology & Evolution 17(4), 183–189.

Lockwood, J. L., P. Cassey, and T. Blackburn (2005). The role of propagule pressure in explaining species invasions. Trends in Ecology & Evolution 20(5), 223–228.

Loreau, M., A. Daufresne, Tand Gonzalez, D. Gravel, F. Guichard, S. J. Leroux, N. Loeuille, F. Massol, and N. Mouquet (2013). Unifying sources and sinks in ecology and earth sciences. Biological Reviews 88(2), 365–379.

MacLean, R. C., A. R. Hall, G. G. Perron, and A. Buckling (2010). The population genetics of antibiotic resistance: integrating molecular mechanisms and treatment contexts. Nature Reviews Genetics 11(6), 405.

Martin, G. (2014). Fisher's geometrical model emerges as a property of complex integrated phenotypic networks. Genetics 197(1), 237–255.

Martin, G., S. F. Elena, and T. Lenormand (2007). Distributions of epistasis in microbes fit predictions from a fitness landscape model. Nature Genetics 39(4), 555.

Martin, G. and L. Roques (2016). The non-stationary dynamics of fitness distributions: Asexual model with epistasis and standing variation. Genetics 204(4), 1541–1558.

Morse, S. S. (2001). Factors in the emergence of infectious diseases. In Plagues and politics, pp. 8–26. Springer.

Pulliam, H. R. (1988). Sources, sinks, and population regulation. The American Naturalist 132(5), 652–661.

Rex Consortium (2013). Heterogeneity of selection and the evolution of resistance. Trends in Ecology & Evolution 28(2), 110–118.

Sokurenko, E. V., R. Gomulkiewicz, and D. E. Dykhuizen (2006). Source-sink dynamics of virulence evolution. Nature Reviews Microbiology 4(7), 548.

Tenaillon, O. (2014). The utility of Fisher's geometric model in evolutionary genetics. Annual Review of Ecology, Evolution, and Systematics 45, 179–201.

Trindade, S., A. Sousa, and I. Gordo (2012). Antibiotic resistance and stress in the light of Fisher's model. Evolution: International Journal of Organic Evolution 66(12), 3815–3824.

Von Holle, B. and D. Simberloff (2005). Ecological resistance to biological invasion overwhelmed by propagule pressure. Ecology 86(12), 3212–3218.